Comparative Study of Different Flexures of MEMS Accelerometers

Avinash Kamble, Siddheshwar Khillare

Abstract—There is a greater demand for developing a monolithic 3- axis accelerometer. The main challenges for developing a 3-axis accelerometer are- the size factor, realizing z-axis sensing, and decoupling the motions of the structure in three mutually perpendicular directions. With this motivation, we analyze structures using different flexures and evaluate their compliance and natural frequencies in three orthogonal directions. In this paper, the analytical and numerical study of different flexures such as straight-beam flexures, crab-leg flexures, serpentine flexures, and folded flexures is done. First, the concept of lumped parameter is described in brief, then numerical simulation of flexures is done using software ANSYS. Finally, a comparison of the analytical and numerical results is presented.

Index Terms—MEMS Accelerometer, Simulink Model.

I. INTRODUCTION

A MEMS accelerometer consists of a proof mass suspended using a compliant flexure anchored to the substrate. A number of micro-accelerometers have been successfully fabricated using surface and bulk micromachining processes [1]. The sensitivity and natural frequency of the accelerometer mainly depend on the type of flexure used. Most MEMS accelerometers are single axis or dual-axes. There is a growing demand for three axes accelerometers especially in some applications such as inertial navigation systems. One way of realizing a 3- axis accelerometer is by assembling two or three accelerometers together. However, these accelerometers have issues such as axes alignment errors and increased size. Alternatively, monolithic 3-axis accelerometers are being developed. Although these accelerometers have either fabrication constraints of thin-film structures (i.e., thickness much smaller than the lateral dimensions), or high cost due to fabrication complexities [2-3] their performance is encouraging. Some monolithic 3-axis accelerometers are actually comprised of individual single-axis sensors with separate proof masses [4], resulting in relatively large sizes. One of the challenges in realizing a 3-axis accelerometer is z-axis sensing. The difficulty of z-axis sensing lies in the making of horizontal electrodes to sense out-of-plane displacement in the presence of large parasitic capacitance on the substrate, especially when differential sensing is needed.

Manuscript published on 28 February 2015.
***** Correspondence Author (s)
Avinash Kamble, Asst. Prof., Department of Mechanical Engineering, NK Orchid College of Engineering and Technology, Solapur, India.
Siddheshwar Khillare, Asst. Prof., Department of Mechanical Engineering, NK Orchid College of Engineering and Technology, Solapur, India.

The z-axis capacitive sensing with torsion spring has been demonstrated [5], but it suffers from either non-differential sensing or complicated fabrication process. Another challenge in designing a 3-axis accelerometer is to decouple the motions of the structure in three mutually perpendicular directions to avoid or reduce the cross-axis sensitivity. This paper evaluates the compliance and natural frequencies of four different types of flexures along three orthogonal directions to assess their feasibility for developing a 3-axis accelerometer. Both analytical and numerical models are presented. Besides, a Simulink® model for a straight beam accelerometer is developed which efficiently evaluates the performance of the accelerometer. In the next section, we discuss the analytical and the numerical procedures for the modal analysis.

II. MODAL ANALYSIS OF DIFFERENT FLEXURES

The modal analysis is done analytically as well as numerically. The dimensions of the proof mass are kept constant and four different flexures, viz., straight, crab-leg, serpentine and folded beam are modelled. The dimensional details of the different flexures used for the modal analysis are given in Table 1. The analytical calculations are done assuming a parallel plate approximation and using lumped parameters [6-7]. Table I: Dimensional details of different flexures used for the modal analysis: the proof mass is 540µm × 400 µm, width of the beam is 2.1 µm and the thickness of all the structures is 3.5 µm.

Table I: Dimensional details of different flexures used for the modal analysis: the proof mass is 540µm × 400 µm, width of the beam is 2.1 µm and the thickness of all the structures is 3.5 µm.

Flexures	Lengths of Beams
Straight	Beam = 300µm
Crab-leg	Thigh = 300 µm
	Shin = 150 µm
Serpentine	No. of meanders = 8
	First and last meanders = 42.9 µm
	Middle six meanders = 32.9 µm
	First and last span beams = 72.9 µm
	Middle five span beams = 147.9 µm
Folded	Truss=400 µm

Published By:
Blue Eyes Intelligence Engineering and Sciences Publication (BEIESP)

	Outer beam=300 µm
	Inner beam=200 µm
	Inner Beam separation =177.9 µm

III. NUMERICAL SIMULATION

Numerical analysis is done using ANSYS 10. The planar structures are discretized using SHELL 93 elements. The density and Young's modulus for polysilicon are taken as 2300 Kg/m3 and 169 GPa, respectively. Fig. (1) shows the mode shapes of four different flexures obtained using ANSYS. The comparison of analytical and numerical calculation is presented in the result and discussion section.

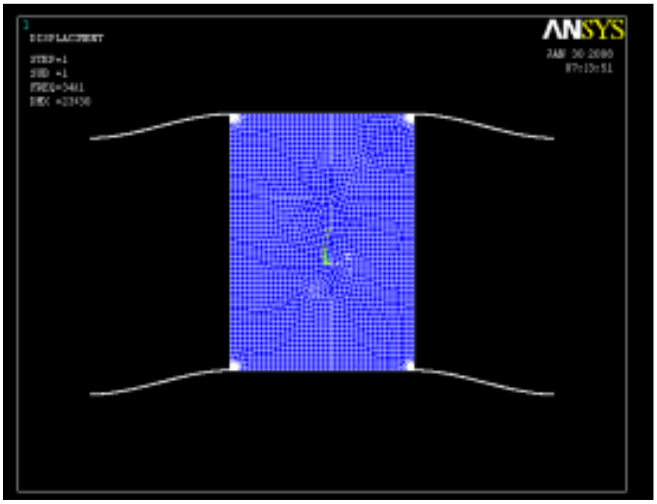

(a)

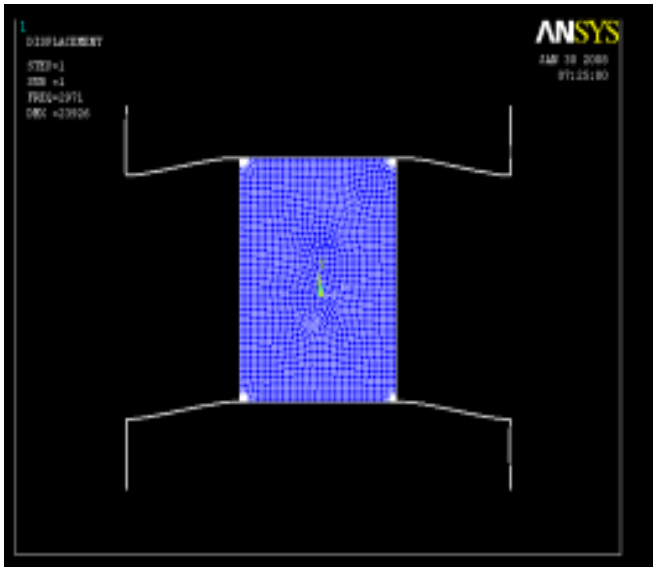

(b)

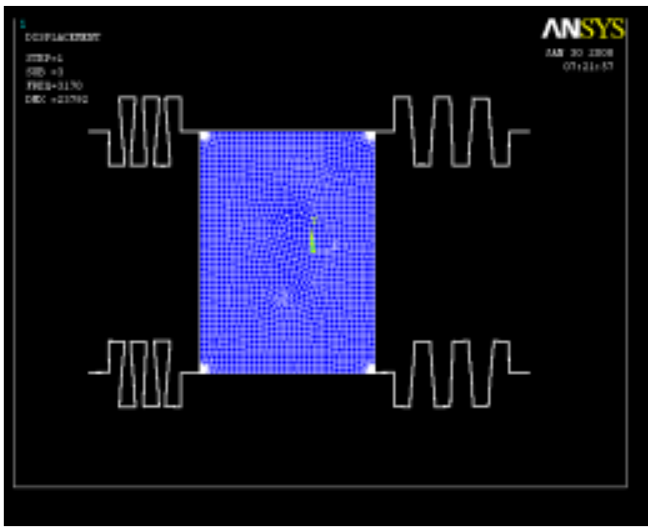

(c)

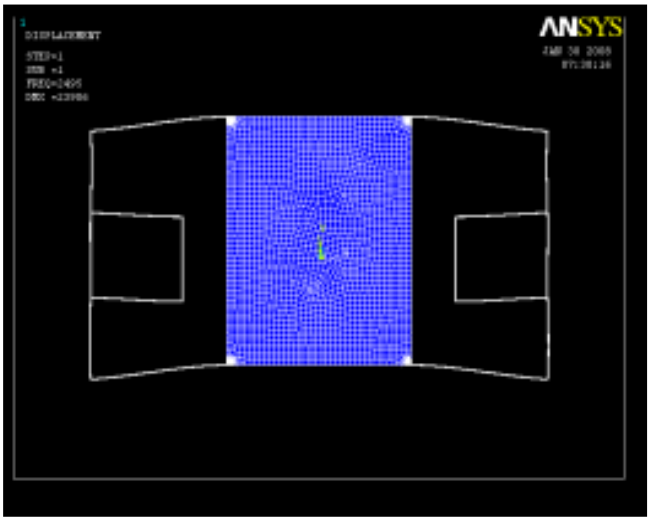

(d)

Fig. 1: Typical mode shapes of different flexures: (a) Straight flexure, (b) Crab-leg flexure, (c) Serpentine flexure, (d) Folded beam flexure

Next, we developed a lumped parameter model to evaluate the overall device sensitivity.

IV. SIMULINK MODEL

Most micromechanical structures can be divided as a discrete combination of mass and spring and modeled using rigid body dynamics. An accelerometer generally consists of a proof mass suspended by compliant beams anchored to a fixed frame. The proof mass m, the suspension beams have an effective spring constant k, and there is a damping coefficient b due to squeeze-film affecting the dynamic movement of the mass. The accelerometer can be modeled by a second-order springmass- damper system, as shown in Fig. (2).

Published By:
Blue Eyes Intelligence Engineering and Sciences Publication (BEIESP)

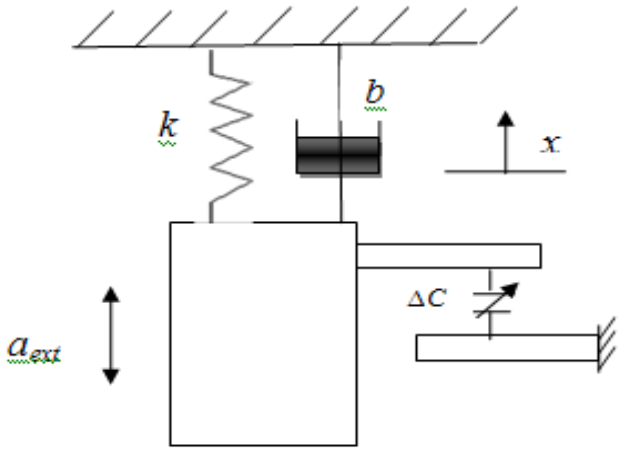

Fig. 2: Lumped parameter model of an accelerometer [8]

The differential equation of the displacement x as a function of input acceleration 'a_{ext}' is given by,

$$\frac{1}{m}(ma_{ext} - b\dot{x} - kx) = \ddot{x} \quad (1)$$

Integration of this signal gives velocity ẋ and displacement (x). Correspondingly, the change in capacitance is obtained as,

$$\Delta C = \frac{\varepsilon A}{g^2}x \quad (2)$$

Where, ε is the permittivity, A is the area of overlap of the comb fingers and g is the air gap between the comb finger. The voltage signal corresponding to the capacitance change is obtained as,

$$\Delta V = \frac{V_{bias}}{C_{bias}}\Delta C \quad (3)$$

Where, V_{bias} is the bias voltage and C_{bias} is the bias capacitance of magnitude 64fF. The Simulink model of the accelerometer with straight beam flexure is shown in Fig. (3)

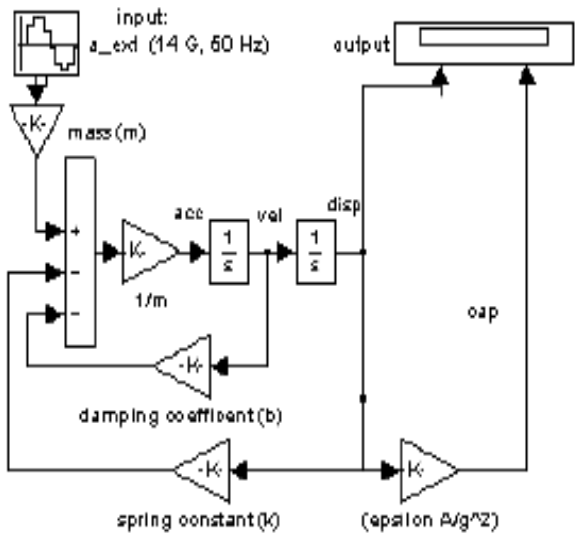

Fig. 3: Lumped parameter model of an accelerometer [8]

V. RESULTS AND DISCUSSION

Table II shows the stiffness of the flexures calculated analytically and numerically.

Table II: Stiffness of the Flexures

Type of beam		Beam Stiffness		% error
		Analytically	(Numerically) k=F/x	
Straight beam	y-axis	0.811	0.811	0
	z-axis	2.19	2.196	0.2732
Crab-leg	x-axis	3.20	3.17	0.9464
	y-axis	0.63	0.61	3.28
	z-axis	0.82	0.71	15.49
Serpentine	x-axis	0.73	0.81	9.88
	y-axis	0.38	0.34	11.76
	z-axis	0.35	0.31	12.9
folded	x-axis	1.50	1.37	9.49
	y-axis	0.28	0.24	16.67
	z-axis	0.51	0.46	10.89

The values of natural frequency calculated analytically as well as numerically are compared in Table III. The excitation acceleration, frequency and the bias voltage are 14 G-50Hz, and 2V, respectively. The displacement of the proof mass and corresponding and capacitance change are shown in Fig. (4). the displacement magnitude is 0.3μm, and corresponding capacitance change is 12.4 fF. The results match well with the experimental results presented in [8].

Table III: Natural frequencies of designed flexures (A = Analytical, N = Numerical, %E = Percentage error)

Natural frequency		Straight	Crab-leg	Serpe-ntine	Fol-ed
f_{nx}	Analytically	---	6842	2821	2465
	Numerically	---	6775	3170	2495
	% Error	---	0.98	11.02	1.19
f_{ny}	Analytically	3431	2960	2093	4452
	Numerically	3431	2971	2194	4539
	% Error	0	0.38	4.58	1.90
f_{nz}	Analytically	5713	2772	1970	2227
	Numerically	5689	3206	2112	2593
	% Error	0.4	13.54	6.72	14.1

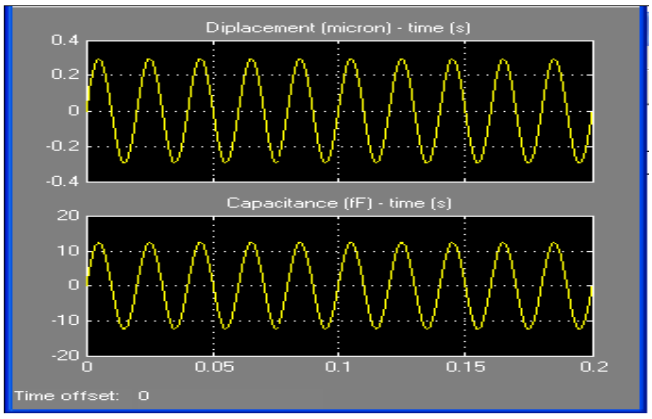

Fig 4: The displacement of the proof mass and corresponding capacitance change and the voltage signal for a 14G 50Hz excitation obtained using lumped parameter Simulink® model.

Published By:
Blue Eyes Intelligence Engineering
and Sciences Publication (BEIESP)

VI. CONCLUSION

The beam stiffness obtained by analytical as well as numerical methods match quite well with a maximum % error of 16.67. The natural frequencies of the lateral (in-plane) and transverse (out-of-plane) oscillations for different flexures obtained analytically using lumped parameters show a very good agreement with those obtained by numerical simulation in ANSYS. The crab-leg flexure is compliant in all the three orthogonal directions. This shows a promise of using this flexure to design a three- axis accelerometer. Further, the lumped parameter simulink model simulates the device performance with fractional efforts in modelling and computation and can be effectively used for device performance optimization.

REFERENCES

[1] Navid Yazdi, Farrokh Ayazi, and Khalil Najafi, "Micromachined Inertial Sensors", proceeding of IEEE, vol. 86, No. 8, August, 1998, pp. 1640-1659.

[2] Hidekuni Takao, Hirofumi Fukumoto, and Makoto Ishida, "A CMOS Integrated Three-Axis Accelerometer Fabricated with commercial Submicrometer CMOS Technology and bulk micromachining", IEEE transactions on electron devices, Vol. 48, 2001, pp. 1961-1669.

[3] R. Toda, N. Takeda, T. Murakoshi, et al.," Electrostatically levitated spherical 3-axis accelerometer", IEEE, 2002, pp. 710-713.

[4] Junseok Chae, Hal and Kulah and Khalil Najafi, " A monolithic three-axis silicon capacitive accelerometer with micro-g resolution", The 12th International Conference on Solid state sensors, Actuators and Microsystem, Boslon, 2003, pp. 81-84.

[5] S. Seok, S. Seong, B. Lee, J. Jim, K. Chum, " A high performance mixed micromachined differential resonant accelerometer", proceeding of IEEE, sensors, Vol. 2, 2002, pp. 1058-1063.

[6] G. K. Fedder, "Simulation of Microelectromechanical systems", Ph. D. dissertation, EECS, University California, Berkeley, 1994.

[7] Suhas Mohite, Nishad Patil and Rudra Pratap, "Design, modeling, and simulation of vibratory micromachined gyroscope", Journal of physics: Conference series 34, 2006, pp. 757-763.

[8] Hao Luo, Gang Zang, L. Richard Carley, Fellow, IEEE, and Garry K. Fedder, "A post-CMOS micromachined lateral accelerometer", Journal of microelectromechanical systems, Vol. 11, No.3, June 2002, pp. 188-195.

Published By:
Blue Eyes Intelligence Engineering and Sciences Publication (BEIESP)